Link to publication

**University of Bath**

**Alternative formats**
If you require this document in an alternative format, please contact:
openaccess@bath.ac.uk

# Baseline-free estimation of residual fatigue life using a third order acoustic nonlinear parameter

Mikael Amura

*Italian Air Force, Flight Test Centre, Airport De Bernardi, Pratica di Mare, Rome, Italy*

Michele Meo[a)] and F. Amerini

*Material Research Centre, Department of Mechanical Engineering, University of Bath, Bath, BA2 7AY, United Kingdom*

Prediction of crack growth and fatigue life estimation of metals using linear/nonlinear acousto-ultrasound methods is an ongoing issue. It is known that by measuring nonlinear parameters, the relative accumulated fatigue damage can be evaluated. However, there is still a need to measure two crack propagation states to assess the absolute residual fatigue life. A procedure based on the measurement of a third-order acoustic nonlinear parameter is presented to assess the residual fatigue life of a metallic component without the need of a baseline. The analytical evaluation of how the cubic nonlinear-parameter evolves during crack propagation is presented by combining the Paris law to the Nazarov–Sutin crack equation. Unlike other developed models, the proposed model assumes a crack surface topology with variable geometrical parameters. Measurements of the cubic nonlinearity parameter on AA2024-T351 specimens demonstrated high sensitivity to crack propagation and excellent agreement with the predicted theoretical behavior. The advantages of using the cubic nonlinearity parameter for fatigue cracks on metals are discussed by comparing the relevant results of a quadratic nonlinear parameter. Then the methodology to estimate crack size and residual fatigue life without the need of a baseline is presented, and advantages and limitations are discussed.
© 2011 Acoustical Society of America. [DOI: 10.1121/1.3621714]

## I. INTRODUCTION

In the last few decades, there has been an extensive amount of research aimed at reducing operative costs for mechanical, civil, and aerospace systems. Aerospace engineering, in particular, is actually trying to optimize maintenance inspections of brand new aircraft as well as to extend the life of old but still valuable assets.[1] In this context, structural damages could lead to catastrophic and expensive failures; therefore the aerospace industry has potentially one of the highest payoffs for structural health monitoring (SHM).

The classical maintenance approach is time consuming and not cost-effective because it is based on inspection of structures at regular interval. In the last decade, novel techniques to be implemented in a SHM concept have been subject to extensive research. SHM can be defined as a system able to detect and interpret adverse "changes" in a structure to improve reliability and reduce life-cycle costs.

Structural health is usually estimated by using a network of transducers that measure and interpret some physical entities such as displacements, accelerations, etc. Sensing methods are usually classified in two categories: passive and active. Passive sensing methods measure data generated from external unknown events even such as crack propagation, impact loading, etc. This method needs a high sensor density because the source is usually unknown and is generally used for detecting acoustic emissions or impact events.[2–4] Active

sensing method relies on a controlled excitation signal collected by a number of sensors. Due to dispersion effects and multimode propagation, the use of a linear guide is complicated in complex structures, being difficult to apply to inhomogeneous materials and in particular to damaged materials where the crack size is comparable with the wavelength. It has been demonstrated that the presence of microcracks, ruptures, and cohesive bonds generates strongly nonlinear dynamic phenomena accompanying the elastic wave propagation.[5,6] These non-linear effects are observed in the course of the degradation process much sooner than any degradation-induced variations of linear parameters (propagation velocity, attenuation, elastic moduli, rigidity, etc.).

In Refs. 5–7, it was shown that nonlinear methods are very sensitive to the progressive degradation of the material structure, and cracks may lead to ultrasonic wave distortion along the wave propagation path and the generation of harmonics of the initial waveform.[8] These phenomena allow using nonlinear ultrasound spectroscopy for early damage detection.[9] These phenomena can be used to monitor the progressive damage progression by analyzing the material nonlinear elastic behavior caused by the presence of cracks,[10–13] These works showed that nonlinear techniques can provide early signs of material degradation long before changes of linear acoustic properties.[6] In the presence of both linear and nonlinear scatterers, *ad hoc* techniques must be developed to discern the presence of linear damage from nonlinear cracks.[14,15]

Nazarov and Sutin[16] proposed a physical model of a medium with cracks to evaluate linear and nonlinear acoustic constants of a fractured medium. They showed that the appearance

[a)]Author to whom correspondence should be addressed. Electronic mail: m.meo@bath.ac.uk

of macrocracks in the material produces large increases in the quadratic, $G_2$, and cubic, $G_3$, nonlinearity parameters. In addition, they highlighted that the cubic nonlinearity parameter should be several orders of magnitude larger than the quadratic. Cantrell[18] applied the Paris–Erdogan[6] equation for crack propagation to the Nazarov–Sutin[16] crack nonlinearity equation to assess the change in $G_2$ as a function of crack growth during the fatigue process, demonstrating that these variations correlate well with the amount of damage. The model proposed by Cantrell assumed constant crack geometrical parameters.

In this paper, we extent the work of Cantrell to the derivation of $G_3$ with (1) constant crack geometrical parameters and (2) crack geometrical parameters varying with the crack size. Comparison between the above-mentioned cases will be presented, and the discussion will also be extended to the quadratic nonlinearity parameters to highlight theoretically the possible advantages of using $G_3$ instead of $G_2$. Then perturbation methods will be used to solve the third order nonlinear wave equation to obtain an expression that could relate the cubic nonlinearity parameter to experimental measurements of the amplitudes of the harmonics evaluated from the frequency spectra of the recorded time domain waveforms. Measurements on AA2024-T351 specimens, containing fatigue fracture of different sizes, will be presented to validate the cubic nonlinearity parameter model. The same measurements will be carried out for the quadratic nonlinearity parameter to compare quantitatively the crack sensitivity of $G_3$ and $G_2$ for the analyzed structure. The proposed approach allows the possibility of determining the residual fatigue life of metallic structures without the need to know a previous material/crack state or baseline, and the procedure to determine it is described with the relative limitations.

## II. CUBIC ORDER NONLINEARITY PARAMETER AS A FUNCTION OF CRACK SIZE

In this section, the relationship between the cubic order nonlinearity parameter and the crack size is derived. The following model is based on the hypothesis of stable propagation fatigue phase, thus the initial nucleation and final failure stages are not taken into account. Nazarov and Sutin[16] derived an expression for the quadratic, $G_2$, and cubic, $G_3$, nonlinearity parameters for non-interacting penny-shaped cracks in bulk material:

$$G_2 = \frac{\beta N_0 G_1^2}{7} \tag{1}$$

$$G_3 = \frac{\gamma N_0 G_1^3 \left[1 - \frac{27 G_1 \beta^2 N_0}{49\gamma}\right]}{9} \tag{2}$$

where,

$$G_1 = \left(1 + \frac{\alpha N_0}{5}\right)^{-1}$$

$N_0$ is the cracks concentration, while $\alpha$, $\beta$, and $\gamma$ are the linear and nonlinear elastic constants of the crack,

$$\alpha = \pi h_s R^2 \left(\frac{E}{\sigma_0}\right)\left(1 + \frac{h_s}{d_0}\right)^{-1} \tag{3}$$

$$\beta = \pi h_s R^2 \left(\frac{E}{\sigma_0}\right)^2 \left(1 + \frac{h_s}{d_0}\right)^{-3} \tag{4}$$

$$\gamma = \pi h_s R^2 \left(\frac{E}{\sigma_0}\right)^3 \left(2 - \frac{h_s}{d_0}\right)\left(1 + \frac{h_s}{d_0}\right)^{-4} \tag{5}$$

$h_s = \sqrt{2}h_0$ where $h_0$ is the characteristic height of the crack surface irregularities, $R$ is the crack radius, $E$ is the Young module, $\sigma_0$ is the internal stress, equal in amplitude but opposite in sign to the external stress and $d_0$ is the distance between the middle lines of the crack surfaces. To derive the cubic nonlinearity parameter as a function of crack growth during the fatigue process, we employ the Paris–Erdogan[19] equation where the variation in the crack radius R is expressed as a function of percent fatigue life to final fracture

$$\frac{dR}{dn} = C\Delta K^m \tag{6}$$

where the material dependent constants $C$ and $m$ are the crack growth intercept and the crack growth exponent, $n$ is the number of fatigue cycles, and $\Delta K$ is the stress intensity range defined by

$$\Delta K = \sigma_0 F(R)\sqrt{\pi R} \tag{7}$$

where $F(R)$ is the shape factor, and it was assumed as a constant in the fatigue stable propagation phase. The derivation of the shape factor $F$, also known as geometry factor, for a circular hole in a plate can be found in Ref. 17 where it is reported how the geometry factor changes when the crack size increases from a circular hole. In detail, for stable crack propagation phase, that behavior is almost constant: for a crack size 5 mm $< a <$ 20 mm, $F$ varies between 1 and 0,8. This justifies the assumption of constant $F$.

Substituting Eq. (7) into Eq. (6), separating the variables and integrating, we obtain an expression for the generic number of fatigue cycles,

$$n = \frac{1}{C[\sigma_0 F\sqrt{\pi}]^m} \int_{R_0}^{R} R^{-m/2} dR. \tag{8}$$

Here $R_0$ is the initial size of the defect. Then the integral calculation leads to the calculation of the total number of cycles n provided by the following equation

$$n = \frac{1}{C[\sigma_0 F\sqrt{\pi}]^m} \left(1 - \frac{m}{2}\right)^{-1} \left(R^{1-m/2} - R_0^{1-m/2}\right). \tag{9}$$

When the size the final crack length is considered, $R_f$, the number of cycles becomes:

$$n_{\text{tot}} = \frac{1}{C[\sigma_0 F\sqrt{\pi}]^m} \left(1 - \frac{m}{2}\right)^{-1} \left(R_f^{1-m/2} - R_0^{1-m/2}\right) \tag{10}$$

The fatigue life percentage can be expressed as the ratio of Eq. (9) to Eq. (10),

$$f = \frac{n}{n_{\text{tot}}} = \frac{\left(R^{1-m/2} - R_0^{1-m/2}\right)}{\left(R_f^{1-m/2} - R_0^{1-m/2}\right)}. \tag{11}$$

Then from Eq. (11) the crack size in function of the fatigue life percentage can be obtained as

$$R = \left[f\left(R_f^{1-m/2} - R_0^{1-m/2}\right) + R_0^{1-m/2}\right]^{(1-m/2)^{-1}} \tag{12}$$

Finally, substituting Eq. (12) into Eq. (2) leads to the evaluation of the cubic nonlinearity parameter as a crack size function. It is straightforward then to evaluate also $G_2$ by substituting Eq. (12) into Eq. (1), obtaining a result similar to Cantrell.[18] $G_3$ and $G_2$ curves as a function of fatigue life are shown in Fig. 1.

Adopting typical material values for AA2024-T35114,[19] the Nazarov-Sutin[16] suggested value of crack-related constants, and some parameters from the used experimental set up:

$$E = 73.1 \times 10^7 \, \frac{\text{g}}{\text{cm}^2}, \quad v = 0.33, \, C = 4,36 \times 10^{-9} \, \frac{\text{cm}}{\text{cycle}},$$
$$m = 3.45, \quad h_s = 10^{-6} \, \text{cm}, \quad d_0 = 3 \times 10^{-6} \, \text{cm},$$
$$N_0 = 2.5 \times 10^{-1} \, \text{cm}^{-3}, \quad \sigma_0 = 3 \times 10^5 \, \frac{\text{g}}{\text{cm}^2},$$
$$R_0 = 5 \times 10^{-6} \, \text{cm}, \quad R_f = 2 \, \text{cm}.$$

$G_3$ and $G_2$ curves have as expected similar trends, and $G_3$ values are about four orders of magnitude higher. This feature highlights that the cubic nonlinearity parameter is more sensitive to cracks and could therefore be preferably used for damage detection and residual life estimation.

## III. FATIGUE CRACK MODEL WITH VARIABLE GEOMETRICAL PARAMETERS

In the previous section, the irregularities of a fatigue fracture surface and the distance between the middle lines of the crack surfaces are assumed constant; however, it should be pointed out that crack geometrical parameters are not constant with damage size but vary with it.[20] Nonetheless it is extremely difficult to find an analytic expression that could consider the complex interactions that take place for each different combination of load, frequency, material, etc. Thus an approximate mathematical model is suggested by taking in account some simply morphological observations: Fatigue fracture surfaces are characterized by subsequent striations,[21] Fig. 2, each of them corresponding to a load cycle.

Such geometrical features could be viewed in section and schematized as isosceles triangles, Fig. 3, that increase in size as the crack grows. Hence the height of the tops of the fracture surface could be estimated as equivalent to 20% of the local spacing between striations[22] and therefore using Eq. (6),

$$H = 0.2C\Delta K^m. \tag{13}$$

Similarly the distance between the middle lines of the fracture surface should be considered variable by using the following equation,[23]

$$d = 16\sigma_0 R \frac{1 - v^2}{3\pi E} \tag{14}$$

where $v$ is the Poisson ratio. By substituting Eqs. (13) and (14) into Eqs. (3), (4), and (5),

$$\alpha = \pi\sqrt{2}(0.2C\Delta K^m)R^2\left(\frac{E}{\sigma_0}\right)\left[1 + \frac{\sqrt{2}(0.2C\Delta K^m)}{\left(16\sigma_0 R \frac{1-v^2}{3\pi E}\right)}\right]^{-1}, \tag{15}$$

$$\beta = \pi\sqrt{2}(0.2C\Delta K^m)R^2\left(\frac{E}{\sigma_0}\right)^2\left[1 + \frac{\sqrt{2}(0.2C\Delta K^m)}{\left(16\sigma_0 R \frac{1-v^2}{3\pi E}\right)}\right]^{-3}, \tag{16}$$

$$\gamma = \pi\sqrt{2}(0.2C\Delta K^m)R^2\left(\frac{E}{\sigma_0}\right)^3\left(2 - \frac{\sqrt{2}(0.2C\Delta K^m)}{\left(16\sigma_0 R \frac{1-v^2}{3\pi E}\right)}\right)$$
$$\times \left[1 + \frac{\sqrt{2}(0.2C\Delta K^m)}{\left(16\sigma_0 R \frac{1-v^2}{3\pi E}\right)}\right]^{-4}, \tag{17}$$
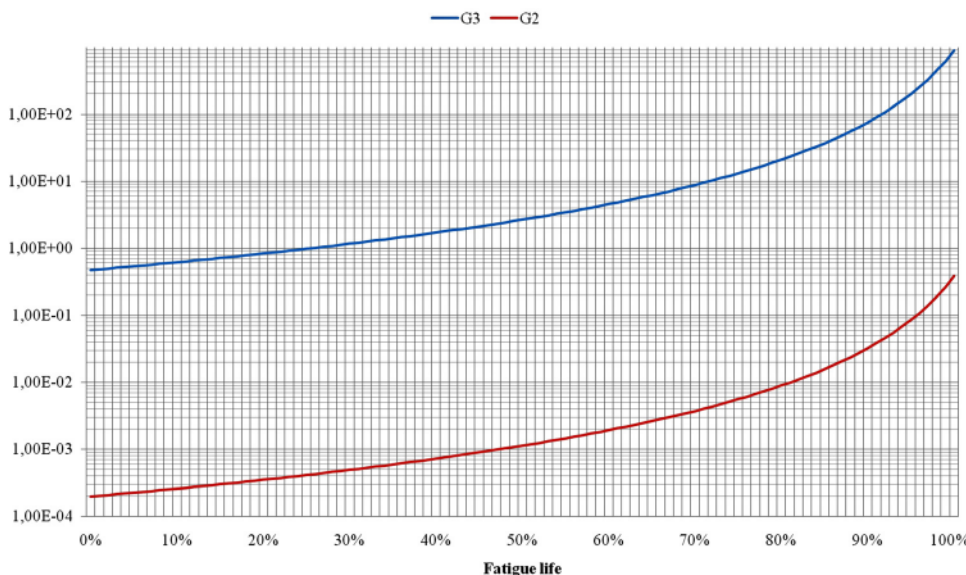


FIG. 1. (Color online) Quadratic nonlinearity parameter, $G_2$ (lower curve), and cubic nonlinearity parameter, $G_3$ (upper curve), plotted as functions of the fatigue life. The model shows that $G_3$ is about four order larger than $G_2$ for almost all the fatigue life.
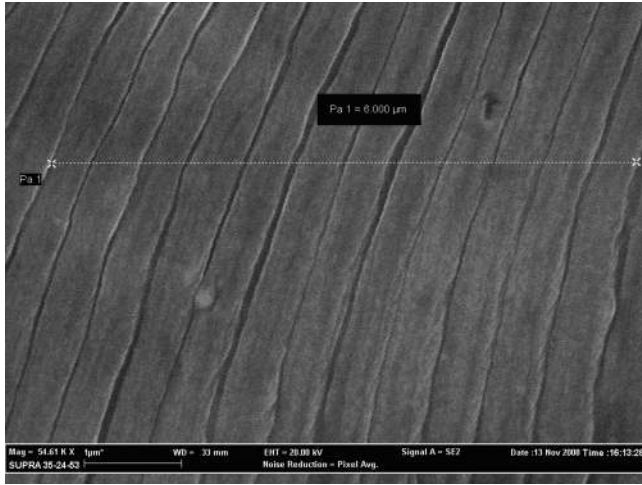
FIG. 2. Typical fatigue striations.



FIG. 3. Fatigue striations model schematization, section view.

where $A_1$ and $A_2$ are, respectively, the frequency amplitudes of first and second harmonics of the recorded time domain waveforms, $k$ is the wavenumber and $a_1$ is the propagation distance. Thus by means of Eq. (18), it is possible to experimentally evaluate the quadratic nonlinearity parameter. A similar approach will be used to find the third order nonlinearity parameter. Starting the nonlinear third order stress strain relationship and substituting it

$$\sigma = E\varepsilon + \frac{EG_2}{2}\varepsilon^2 + \frac{EG_3}{6}\varepsilon^3 \qquad (19)$$

in the nonlinear wave equation,

$$\rho\frac{\partial^2 u}{\partial t^2} = \frac{\partial \sigma}{\partial a_1} \qquad (20)$$

where $\varepsilon = \partial u/\partial a_1$ is the strain and $\rho$ is the material density leads to

$$\frac{\partial^2 u}{\partial t^2} - c^2\frac{\partial^2 u}{\partial a_1^2} = c^2\left(G_2\frac{\partial u}{\partial a_1}\frac{\partial^2 u}{\partial a_1^2} + \frac{G_3}{2}\left(\frac{\partial u}{\partial a_1}\right)^2\frac{\partial^2 u}{\partial a_1^2}\right), \qquad (21)$$

where $c = \sqrt{E/\rho}$ is the wave speed. Equation (21) can be solved using the perturbation method that admits the general solution,

$$u = u^{(1)} + u^{(2)} + u^{(3)} + \cdots \qquad (22)$$

A solution of the Eq. (21) at $a_1 = 0$ is

$$u^{(1)} = u_1\, sin(ka_1 - \omega t). \qquad (23)$$

it is finally possible to predict theoretically $G_2$ and $G_3$ for variable geometrical crack parameters (VGCP) using Sec. II findings, Figs. 4 and 5.

These were compared to the results of Fig. 1, $G_3$ and $G_2$ as calculated with constant geometric parameters. Considering the VGCP model, $G_3$ and $G_2$ values are lower during almost all the propagation except for the last part when the unstable rupture is approaching. Also in the VGCP model the distance between $G_3$ and $G_2$ remains constant at about four orders of magnitude, confirming that measures of $G_3$ could lead to a greater sensibility.

## IV. DERIVATION OF THE THIRD ORDER NONLINEARITY PARAMETERS

Cantrell[23] used the second order solution approximation of the non linear wave equation to obtain the following expression of the quadratic nonlinearity parameter,

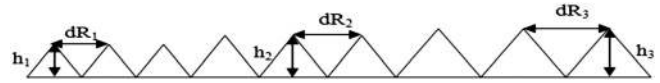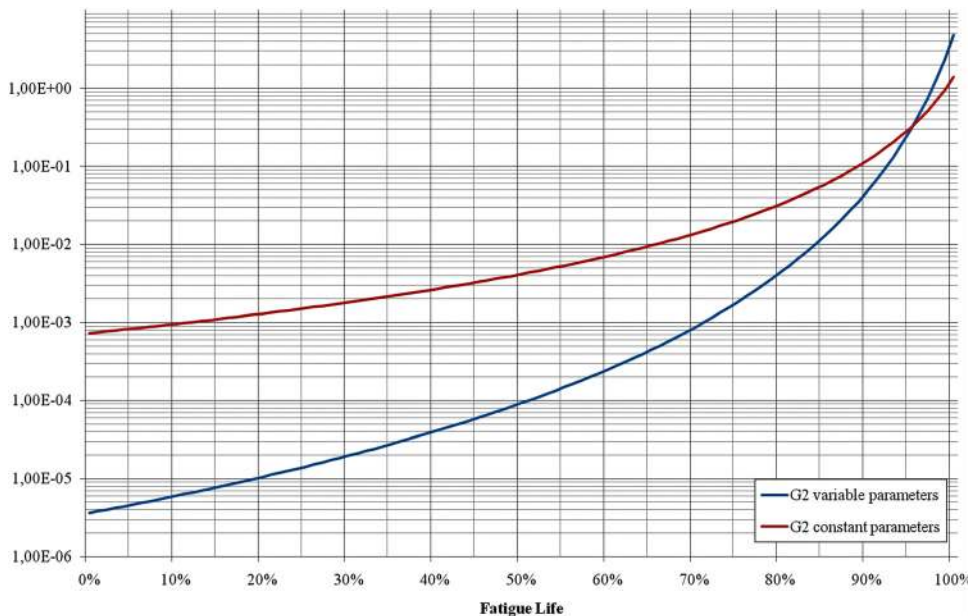$$G_2 = \frac{8A_2}{A_1^2 k^2 a_1}, \qquad (18)$$



FIG. 4. (Color online) $G_2$ model comparisons: constant geometrical crack parameters and variable geometrical crack parameters.
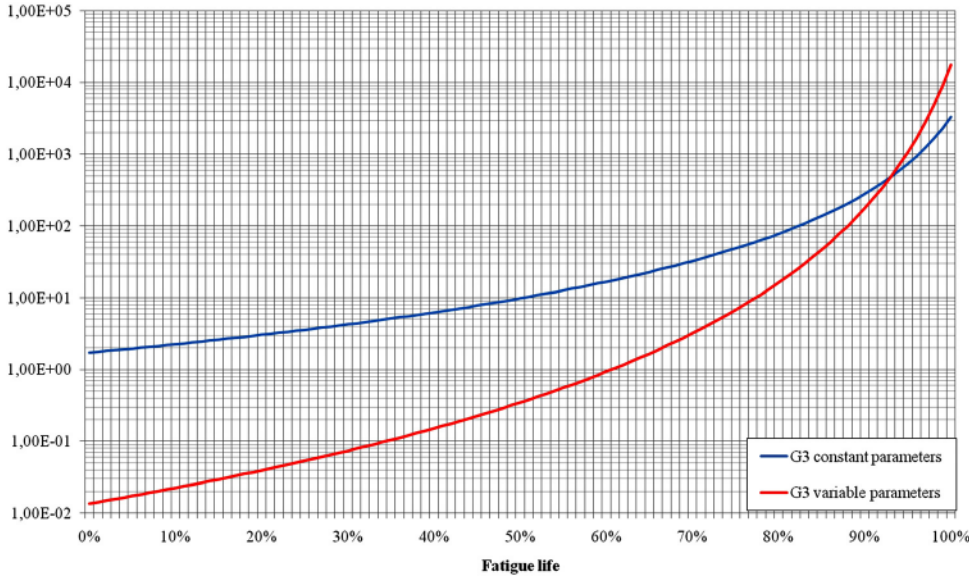
FIG. 5. (Color online) $G_3$ model comparisons: constant geometrical crack parameters and variable geometrical crack parameters.

Considering now only the contribution to the second order of the Eq. (21),

$$\frac{\partial^2 u}{\partial t^2} - c^2 \frac{\partial^2 u}{\partial a_1^2} = c^2 G_2 \frac{\partial u}{\partial a_1} \frac{\partial^2 u}{\partial a_1^2}. \qquad (24)$$

Substituting Eq. (23) into the right side of the Eq. (24), we obtain,

$$\frac{\partial^2 u^{(2)}}{\partial t^2} - c^2 \frac{\partial^2 u^{(2)}}{\partial a_1^2} = -\frac{c^2 u_1^2}{2} G_2 k^3 \sin 2(ka_1 - \omega t). \quad (25)$$

Solution to the Eq. (25) is obtained by assuming a general solution in the following form,[24]

$$u^{(2)} = f(a_1) \sin 2(ka_1 - \omega t) + g(a_1) \cos 2(ka_1 - \omega t). \qquad (26)$$

Substituting Eq. (26) in the left side of the Eq. (25),

$$\left( -4k \frac{dg}{da_1} + \frac{d^2 f}{da_1^2} \right) \sin 2(ka_1 - \omega t)$$
$$+ \left( \frac{d^2 g}{da_1^2} + 4k \frac{df}{da_1} \right) \cos 2(ka_1 - \omega t)$$
$$= -\frac{u_1^2}{2} G_2 k^3 \sin 2(ka_1 - \omega t). \qquad (27)$$

By equating coefficients of the sinusoidal terms in Eq. (27), we obtain,

$$-\left( 4k \frac{dg}{da_1} - \frac{d^2 f}{da_1^2} \right) = \frac{u_1^2}{2} G_2 k^3. \qquad (28)$$

$$\left( \frac{d^2 g}{da_1^2} + 4k \frac{df}{da_1} \right) = 0. \qquad (29)$$

Assuming that $d^2 g / da_1^2 = 0$ and $df / da_1 = 0$, turns Eqs. (28) and (29) into consistent solution that leads to the determination of

$$u^{(2)} = -\frac{u_1^2 k^2}{8} a_1 G_2 \cos 2(ka_1 - \omega t). \qquad (30)$$

Now $u^{(3)}$ will be evaluated by repeating the same process for the third order. Thus, considering the third order contribution to the nonlinear wave equation,

$$\frac{\partial^2 u}{\partial t^2} - c^2 \frac{\partial^2 u}{\partial x^2} = c^2 \frac{G_3}{2} \left( \frac{\partial u}{\partial x} \right)^2 \frac{\partial^2 u}{\partial x^2} \qquad (31)$$

and substituting Eq. (23) into the right side of the Eq. (31),

$$\frac{\partial^2 u}{\partial t^2} - c^2 \frac{\partial^2 u}{\partial x^2} = -c^2 \frac{G^3}{8} u_1^3 k^4$$
$$\times [\sin(ka_1 - \omega t) + \sin 3(ka_1 - \omega t)]. \quad (32)$$

The solution to Eq. (32) is obtained by assuming a general solution in the following form,

$$u^{(3)} = w(a_1) \sin 3(ka_1 - \omega t) + y(a_1) \sin(ka_1 - \omega t)$$
$$+ q(a_1) \cos 3(ka_1 - \omega t) + p(a_1) \cos(ka_1 - \omega t). \qquad (33)$$

Substituting Eq. (33) into the left side of the Eq. (32),

$$-\left[ \frac{dw}{da_1} 6k \cos 3(ka_1 - \omega t) - \frac{dq}{da_1} 6k \sin 3(ka_1 - \omega t) \right.$$
$$+ \frac{d^2 w}{da_1^2} \sin 3(ka_1 - \omega t) + \frac{d^2 q}{da_1^2} \cos 3(ka_1 - \omega t)$$
$$+ \frac{dy}{da_1} 2k \cos(ka_1 - \omega t) - \frac{dp}{da_1} 2k \sin(ka_1 - \omega t)$$
$$+ \left. \frac{d^2 y}{da_1^2} \sin(ka_1 - \omega t) + \frac{d^2 p}{da_1^2} \cos(ka_1 - \omega t) \right]$$
$$= -\frac{G_3}{8} u_1^3 k^4 [\sin 3(ka_1 - \omega t) + \sin(ka_1 - \omega t)]. \qquad (34)$$

By equating coefficients of the sinusoidal terms in Eq. (34), it can be followed that

$$\frac{dy}{da_1}2k + \frac{d^2p}{da_1^2} = 0, \tag{35}$$

$$\frac{dp}{da_1}2k - \frac{d^2y}{da_1^2} = \frac{G_3}{8}u_1^3k^4, \tag{36}$$

$$-\frac{dw}{da_1}6k - \frac{d^2q}{da_1^2} = 0, \tag{37}$$

$$\frac{dq}{da_1}6k - \frac{d^2w}{da_1^2} = -\frac{G_3}{8}u_1^3k^4. \tag{38}$$

Assuming that $d^2p/da_1^2 = 0$, $dy/da_1 = 0$, $d^2q/da_1^2 = 0$, and $dw/da_1 = 0$, allows us to evaluate $q(a_1)$ and $p(a_1)$ as,

$$p = -\frac{G_3}{16}u_1^3k^3a_1, \tag{39}$$

$$q = -\frac{G_3}{48}u_1^3k^3a_1. \tag{40}$$

Using Eqs. (22), (23), (30), (39), and (40), it is possible to build the third order solution of the nonlinear wave equation,

$$u = u_1\sin(ka_1 - \omega t) - \frac{u_1^2k^2}{8}a_1 G_2\cos2(ka_1 - \omega t)$$
$$- \frac{G_3}{16}u_1^3k^3a_1\left[\frac{1}{3}\cos3(ka_1 - \omega t) + \cos(ka_1 - \omega t)\right]. \tag{41}$$

Equation (38) provides a relation between the experimental measurement of the frequency spectra harmonics of the recorded time domain waveforms and the solution of the Eq. (18), indeed,

$$A_1 = u_1 - \frac{G_3}{16}u_1^3k^3a_1, \tag{42}$$

$$A_2 = -\frac{u_1^2k^2}{8}a_1G_2, \tag{43}$$

$$A_3 = -\frac{G_3}{48}u_1^3k^3a_1. \tag{44}$$

Equations (42) and (44) suggest that, considering $A_1 \approx u_1$, $G_3$ may be obtained as

$$G_3 \approx \frac{A_3}{A_1^3}\frac{48}{k^3a_1}. \tag{45}$$

Then using Eq. (45), it is possible to experimentally assess the cubic nonlinearity parameter and validate the model presented in Sec. II.

## V. EXPERIMENTAL VALIDATION

Five AA2024-T351 specimens were fatigued at a rate of 10 Hz under uniaxial, stress-controlled load at 10 KN and stress ratio $\sigma_{\min}/\sigma_{\max} = 0$. The geometry of the samples with four holes is shown in Fig. 6. To initiate fatigue the crack, 500 $\mu$m notches were made in correspondence to the hole no. 1 in direction of the hole no. 2. The ultrasound wave propagation area is 3 mm thick.

Purely sinusoidal ultrasonic waves of amplitude 30 Vpp (amplified from 10 Vpp) and frequency 5 MHz were used and recorded using a 1 cm diameter piezoelectric transducer. The signal generation was performed by a TTI 1200 series signal generator. Signals were recorded by Picoscope 4000 series digital oscilloscope. Time-domain and frequency domain signals were obtained by Picoscope relevant software.

Measurements of $G_2$ and $G_3$ were made in the manner described in Sec. IV. at five different crack lengths: 2, 5, 10, 15, and 20 mm, corresponding to 67%, 86%, 94%, 97%, and ~100% of the fatigue life and, respectively, to 10%, 25%, 50%, 75%, and ~100% of damage; therefore the initiation stage represents, as expected, the preponderance of the fatigue lifetime.[25] Results are presented in Figs. 7 and 8 and are compared with the models proposed.

Thus experimental data show good agreement with theoretical models, confirming the predicted higher values of $G_3$ in comparison to $G_2$, therefore making the cubic nonlinearity parameter preferable for higher sensitivity to fatigue crack. Moreover, constant parameter model seems to describe adequately $G_3$ and $G_2$ progression up 50% of damage, then the VGCP model highlights a better agreement to the experimental data.

In particular, the experimental data show that good agreement with CGCP model in the initial propagation phase until 25% of the crack size for the $G_3$ while about 50% for $G_2$. In the last phase of the crack propagation stage, the experimentally measured CGCP model of $G_2$ and $G_3$ underestimates the model derived. On the other hand, the VCGP
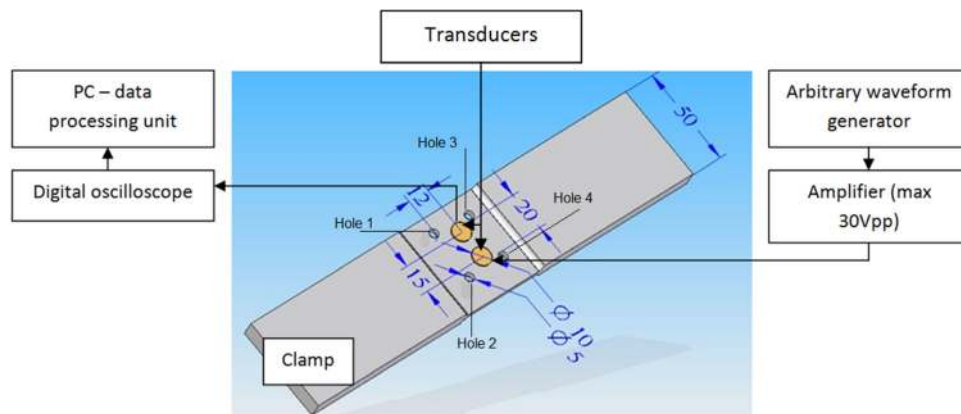


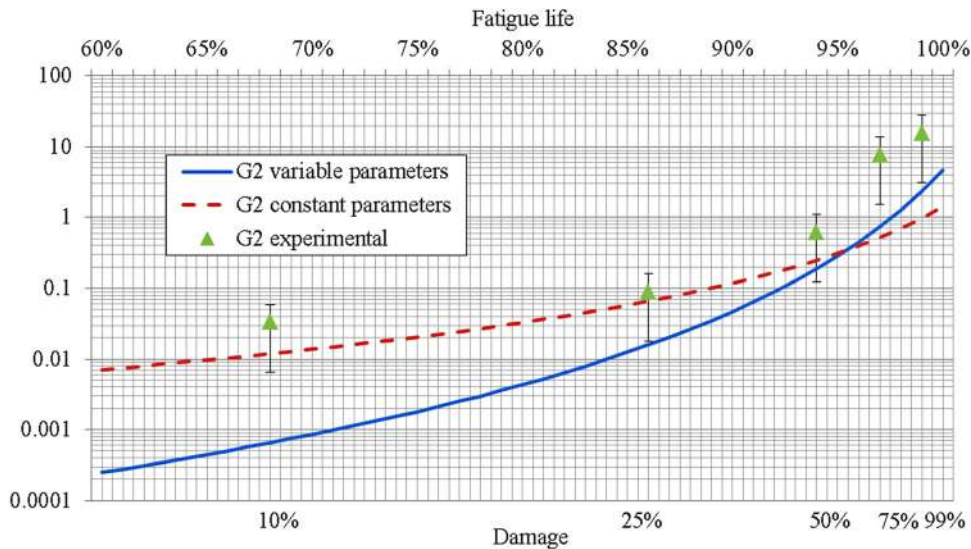FIG. 6. (Color online) Specimens geometry and experimental setup, dimensions in mm.

1834    J. Acoust. Soc. Am., Vol. 130, No. 4, October 2011

Amura *et al.*: Baseline-free estimation fatigue life

FIG. 7. (Color online) Experimental results and model predictions for $G_2$.

model underestimates the initial propagation phase; however, it better describes the final propagation stage of the rupture mechanism with a very good correlation. This is more pronounced for $G_2$ than $G_3$ model.

This excellent correlation shows that it is possible by using the CGCP and VGCP models to estimate the remaining fatigue life by measuring experimentally measuring the $G_2$ and $G_3$ as discussed in the following section.

## VI. RESIDUAL LIFE PROCEDURE

The procedure to estimate the residual life of a metallic structure is as follows (Fig. 9):

(1) Estimate the type of fatigue loading of the component, i.e., $\sigma_{min}/\sigma_{max}$.
(2) Measure the crack size in function of the fatigue life percentage using the following equation

$$R = \left[ f\left( R_f^{1-m/2} - R_0^{1-m/2} \right) + R_0^{1-m/2} \right]^{(1-m/2)^{-1}}.$$

(3) Use the following equation to obtain the theoretical quadratic and cubic nonlinearity curve as a function of crack size and fatigue life,

$$G_2 = \frac{\beta N_0 G_1^2}{7} \quad \text{and} \quad G_3 = \frac{\gamma N_0 G_1^3 \left[ 1 - \dfrac{27 G_1 \beta^2 N_0}{49 \gamma} \right]}{9}.$$

(4) Then measure experimentally the second and third order nonlinearity parameter. Then using the curve shown in the following text, enter the measured value to get an estimation of the residual fatigue life and crack size.

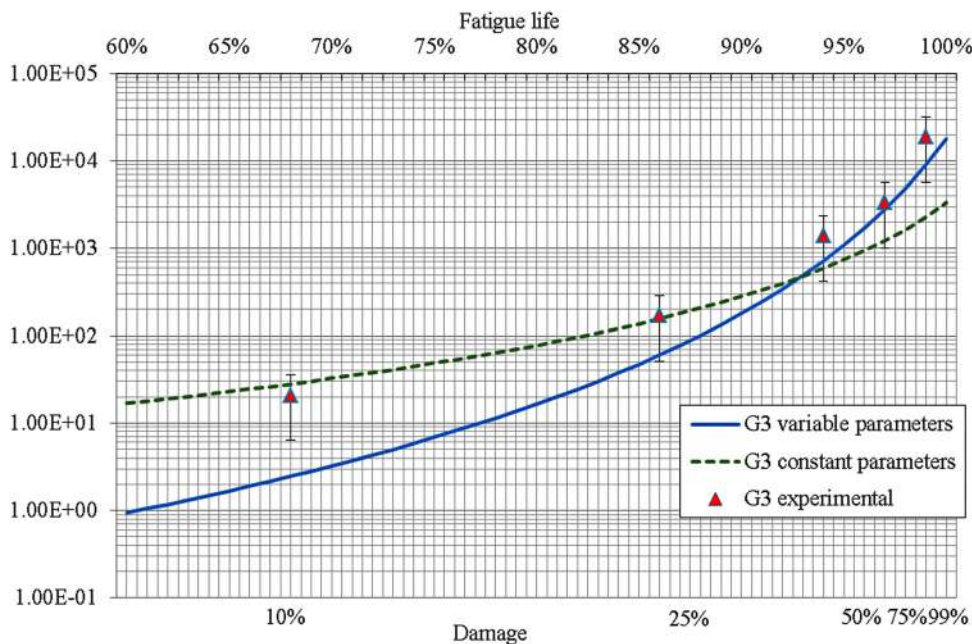The proposed approach has clearly some limitations that are discussed in the following text.



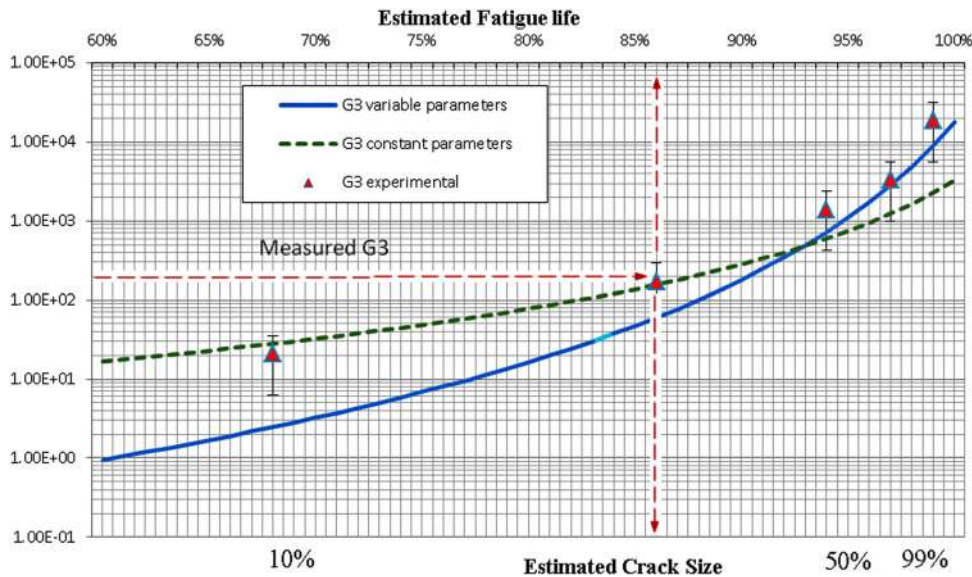FIG. 8. (Color online) Experimental results and model predictions for $G_3$.

FIG. 9. (Color online) Residual life and crack size estimation.

(1) For the structure investigated, the crack locations was known. Therefore this approach is suitable to assess residual life of a hot-spot where the location and possibly the crack propagation direction is known.

(2) The cyclic loading was defined, and consequently the stress experienced by the material. However, real life structures experience random and unknown loads, and therefore the value of the measured nonlinearity parameter could differ from the theoretical value calculated using a zero $\sigma_{min}/\sigma_{max}$ ratio.

(3) Because the amplitude of the second and third order harmonics are smaller than the excitation signal, the presence of material attenuation and equipment noise could yield an unclear signal, therefore the sensors should be located within a sensible distance from the actual crack location. Moreover, high signal amplification may be needed.

(4) The present model is valid for non-interacting crack, therefore the presence of multiple cracks, crack branching, etc., cannot in principle be used with this approach, and new methods are needed to be developed to cope with these failure cases.

(5) For some materials, the value of the third harmonic may be much smaller than the second harmonic. This poses significant challenges on the experimental equipment to be used. However, for material with hysteretic type of damage, this approach would be preferable because the material may generate only third harmonics.

(6) Because the initial nucleation phase and final breakdown phases are not taken into account in this procedure, the relationship between the quadratic and cubic nonlinearity and crack size/fatigue life is valid mainly for the fatigue stable propagation phase.

## VII. CONCLUSIONS

In this paper, a procedure is presented to predict the residual fatigue life and crack propagation of a metallic structure using nonlinear guided waves. The method is based on the measurement of the third order acoustic nonlinearity. A mathematical derivation was presented to estimate the cubic and quadratic nonlinearity parameter by combining the Paris law to the Nazarov–Sutin crack nonlinearity equation for cracks that evolve during fatigue mechanisms in metals with variable and constant crack geometrical parameters hypothesis.

Experimental tests conducted on AA2024-T351 specimens, containing fatigue fracture of different lengths, showed very good correlation was obtained for the CGCP model up to 50% crack size for $G_2$ and 25% for the $G_3$ parameter. The VCGP provided better correlation in the final phase of the crack propagation. The results showed different order of magnitude of $G_2$ and $G_3$. The latest parameter possesses a higher sensitivity than $G_2$ making it a better experimental parameter to measure fatigue life.

The overall results showed clearly that by measuring the $G_3$ nonlinearity parameters, it is possible to estimate crack size and residual fatigue life. Finally, advantages and limitations of the procedure were also discussed.

[1]M. Amura, F. De Trane, and L. Aiello, *Constant speed drive—time between overhaul extension: a case study from Italian Air Force Fleet.* NATO RTO MP Applied Vehicle Technology 157 Symposium (2008).

[2]M. Meo, G. Zumpano, M. Piggot, and G. Marengo, "Impact identification on a sandwich plate from wave propagation responses," Compos. Struct. **71**(3-4), 302-306 (2005).

[3]F. Ciampa and M. Meo, "Acoustic emission source localization and velocity determination of the fundamental mode $A_0$ using wavelet analysis and Newton-based optimization technique," Smart Mater. Struct. **19**(4), 045027 (2010).

[4]F. Ciampa and M. Meo, "A new algorithm for acoustic emission localization and flexural group velocity determination in anisotropic structures," Composites, Part A **41**(12), 1777–1786 (2010).

[5]M. Meo and G. Zumpano, "Nonlinear elastic wave spectroscopy identification of impact damage on a sandwich plate," Composite. Struct. **71**, 469–474 (2005).

[6]J. H. Cantrell, "Quantitative assessment of fatigue damage accumulation in wavy slip metals from acoustic harmonic generation," Philos. Mag. **86**(11), 1539–1554 (2006).

[7]M. Meo and G. Zumpano, "A new nonlinear elastic time reversal acoustic method for the identification and localisation of stress corrosion cracking in welded plate-like structures—A simulation study," Int. J. Solids Struct. **44**, 3666, (2007).

[8]C. Pecorari, "Nonlinear interaction of plane ultrasonic waves with an interface between rough surfaces in contact," J. Acoust. Soc. Am. **113**(6), 3065–3072 (2003).

[9]M. Meo, U. Polimeno, and G. Zumpano, "Detecting damage in composite material using onlinear elastic wave spectroscopy methods," Appl. Compos. Mater. **15**(3), 115–126 (2008).

[10]G. Zumpano and M. Meo, "Damage localization using transient non-linear elastic wave spectroscopy on composite structures," Int. J. Non-Linear Mech. **43**(3), 217–230 (2008).

[11]M. Meo, U. Polimeno, and G. Zumpano, "Detecting damage in composite material using nonlinear elastic wave spectroscopy methods," Appl. Compos. Mater. **15**, 115–1126 (2008).

[12]G. Zumpano and M. Meo, "A new damage detection technique based on wave propagation for rails," Int. J. Solids Struct. **43**, 1023–1046 (2006).

[13]U. Polimeno, M. Meo, D. Almond, and S. Angioni, "Detecting low velocity impact damage in composite plate using nonlinear acoustic methods," Appl. Compos. Mater. **17**(5), 481–488 (2010).

[14]E. Barbieri and M. Meo, "Time reversal DORT method applied to nonlinear elastic wave scattering," Wave Motion **47**(7), 452–467 (2010).

[15]E. Barbieri and M. Meo, "Discriminating linear from nonlinear elastic damage using a nonlinear time reversal DORT method," Int. J. Solids Struct. **47**(20), 2639–2652 (2010).

[16]K. Van Den Abeele, "Multi-mode nonlinear resonance ultrasound spectroscopy for defect imaging: An analytical approach for the one-dimensional case," J. Acoust. Soc. Am. **122**(1), 73–90 (2007).

[17]V. E. Nazarov and A. M. Sutin, "Nonlinear elastic constants of solids with cracks," J. Acoust. Soc. Am. **102**, 3349 (1997).

[18]Fatigue and fracture, stress intensity factor appendix, in *ASM Handbook* (ASM International, 1996), Vol. 19, pp. 170–176.

[19]P. C. Paris and F. Erdogan, "A critical analysis of crack propagation laws," Trans. ASME J. Basic Eng. **85**, 528 (1963).

[20]ASTM STP738: *Fatigue Crack Growth Measurement and Data Analysis* (American Society for Testing and Materials, 1981), p. 22.

[21]P. Lukáš, "Fatigue crack nucleation and microstructure," in *ASM Handbook 19. Fatigue and Fracture* (ASM International, 1996), Vol. 19, pp. 96–109.

[22]L. Allegrucci, M. Amura, F. Bagnoli, and M. Bernabei, "Fatigue fracture of a aircraft canopy lever reverse," Eng. Failure Anal. **16**, 391–401 (2009).

[23]K. Furukawa, Y. Murakami, and S. Nishida, "A method for determining stress ratio of fatigue loading from the width and height of striation," Int. J. Fatigue **20**(7), 509–516 (1998).

[24]J. H. Cantrell, "Fundamentals and applications of non-linear ultrasonic nondestructive evaluation," in *Ultrasonic Non-Destructive Evaluation*, edited by K. Tribikram (CRC Press, Boca Raton, FL, 2004), Vol. 6, pp. 363–434.

[25]A. A. Shah and Y. Ribakov, "Non-linear ultrasonic evaluation of damaged concrete based on higher order harmonic generation," Mater. Des. **30**, 4095–4102 (2009).